RESEARCH ARTICLE

Utilisation of the Prestwick Chemical Library to identify drugs that inhibit the growth of mycobacteria

Panchali Kanvatirth[1¤], Rose E. Jeeves[2], Joanna Bacon[2], Gurdyal S. Besra[1], Luke J. Alderwick[1] *

1 Institute of Microbiology and Infection, School of Biosciences, University of Birmingham, Birmingham, United Kingdom, 2 TB Research Group, National Infection Service, Public Health England, Porton Down, Salisbury, United Kingdom

¤ Current address: Department of Veterinary Medicine, University of Cambridge, Cambridge, United Kingdom.
* l.alderwick@bham.ac.uk

Abstract

Tuberculosis (TB) is an infectious bacterial disease that kills approximately 1.3 million people every year. Despite global efforts to reduce both the incidence and mortality associated with TB, the emergence of drug resistant strains has slowed any progress made towards combating the spread of this deadly disease. The current TB drug regimen is inadequate, takes months to complete and poses significant challenges when administering to patients suffering from drug resistant TB. New treatments that are faster, simpler and more affordable are urgently required. Arguably, a good strategy to discover new drugs is to start with an old drug. Here, we have screened a library of 1200 FDA approved drugs from the Prestwick Chemical library using a GFP microplate assay. Drugs were screened against GFP expressing strains of *Mycobacterium smegmatis* and *Mycobacterium bovis* BCG as surrogates for *Mycobacterium tuberculosis*, the causative agent of TB in humans. We identified several classes of drugs that displayed antimycobacterial activity against both *M. smegmatis* and BCG, however each organism also displayed some selectivity towards certain drug classes. Variant analysis of whole genomes sequenced for resistant mutants raised to florfenicol, vanoxerine and pentamidine highlight new pathways that could be exploited in drug repurposing programmes.

Introduction

Tuberculosis (TB) remains a major global health issue, despite it being over twenty years since the World Health Organisation (WHO) declared TB a global emergency [1]. In 2016, TB killed around 1.3 million people and now ranks alongside HIV as the leading cause of death globally. It has been estimated that almost 6.3 million new cases of TB are to have occurred in 2016; 46% of these new TB cases were individuals co-infected with HIV. Alarmingly, an estimated 4.1% of new TB cases and 19% of previously treated TB cases are infections caused by Multi-

Drug Resistant TB (MDR-TB), and in 2016 an estimated 190,000 people died from this form of the disease. Furthermore, extensively drug-resistant TB (XDR-TB) has now been reported in 105 countries, and accounts for approximately 30,000 TB patients in 2016. If these numbers are to reduce in line with milestones set by the WHO End TB Strategy, alternative therapeutic agents that target novel pathways are urgently required.

Drug repurposing (or drug redeployment), is an attractive approach for the rapid discovery and, in particular, development of new anti-TB drugs [2–5]. Due to the time and cost of bringing new molecular entities through the developmental pipeline to clinic, drug repurposing offers an expedient option, in part due to pre-existing pharmacological and toxicological data-sets that allow for rapid profiling of active hits [6]. In this study, we used GFP-expressing strains of *M. smegmatis* and *Mycobacterium bovis* BCG (henceforth, BCG) in order to screen the Prestwick Chemical Library for antimycobacterial drugs. Together with drugs that have previously been identified from similar screens [7], we identified a number of novel hits that display good antimycobacterial activity which were also confirmed in *Mycobacterium tuberculosis* H37Rv. We sought to characterise the mode of action of selection of hits, by performing whole genome sequencing with variant analysis on laboratory resistant mutants supported by target engagement studies. This study highlights both the usefulness and circumspection required when utilising *M. smegmatis* and BCG in drug repurposing screens to identify new anti-TB agents.

Materials and methods

Bacterial strains, plasmids and growth media

M. smegmatis mc^{2}155 was electroporated with pSMT3-eGFP and transformants were selected on Tryptic Soy Agar supplemented with hygromycin B (20 μg/ml). Single colonies were used to inoculate 10 mL of Tryptic Soy Broth supplemented with Tween 80 (0.05% v/v) at 37˚C with shaking at 180 rpm. *M. smegmatis* mc^{2}155 harbouring pSMT3-eGFP was diluted 1/100 into Middlebrook 7H9 supplemented with glycerol (2 mL/L) and Tween 80 (0.05% v/v) and further sub-cultured at 37˚C with shaking at 180 rpm. *M. bovis* BCG Pasteur strain was electroporated with pSMT3-eGFP and transformants selected on Middlebrook 7H10 containing OADC (10% v/v) and hygromycin B (20 μg/ml). Single colonies were inoculated into 50 mL of Middlebrook 7H9 containing OADC (10% v/v) and Tween 80 (0.05% v/v) and statically cultured at 37˚C for ~ 5 days. Both *M. smegmatis* mc^{2}155 and BCG expressing eGFP were quantified by sampling 200 μL of cells which were 2-fold serially diluted across a black F-bottom 96-well micro-titre plate and fluorescence was measured using a BMG Labtech POLARstar Omega plate reader (Excitation 485–12 nm, Emission 520 nm).

Validation of eGFP reporter screen

Batch cultures of *M. smegmatis* pSMT3-eGFP and BCG pSMT3-eGFP were adjusted to give a basal reading of 20,000 Relative Fluorescent Units (RFU) by diluting into fresh Middlebrook 7H9 containing Tween 80 (0.05% v/v) with additional OADC (10% v/v) for BCG (final well volume of 200 μL). The anti-mycobacterial drugs isoniazid, ethambutol, streptomycin, pyrazinamide and rifampicin were included in over a range of concentrations on assay plates. Wells containing mycobacterial culture in the presence of 1% DMSO represent high controls, whilst wells containing only media constitute low controls. Assay plates were cultured for 48 hours in a Thermo Cytomat plate-shaker incubator (100% humidity at 37˚C with 180 rpm plate agitation) and eGFP fluorescence was measured kinetically every 2 hours.

Medium throughput screen of the Prestwick Chemical Library

The Prestwick Chemical Library (1200 drugs) was purchased from Specs.net preformatted in master plates so that all compounds were solubilized in 100% DMSO at a final concentration of 10 mM. A fully automated Hamilton Star work-station was used for all liquid handling protocols. Compounds were loaded into black F-bottom 96-well assay ready plates (Greiner) followed by 200 μL of either *M. smegmatis* pSMT3-eGFP or BCG pSMT3-eGFP resulting in a final drug concentration of 20 μM in the primary screen. Wells containing only cells (high control) or cells in combination with 50 μg/mL rifampicin (Sigma) (low control) were included on each assay plate to establish positive and negative controls, respectively. Assay plates were cultured at for 48 hours in a Thermo Cytomat plate-shaker incubator (100% humidity at 37°C with 180 rpm plate agitation) and eGFP fluorescence was measured kinetically every 2 hours to generate growth curves for individual wells of each assay plate. Data from the final 48 hr read was normalized using the following equation:

$$\%Survival = \left(\frac{x - \bar{x}\,(\text{negative controls})}{\bar{x}\,(\text{positive controls}) - \bar{x}\,(\text{negative controls})} \right) \times 100$$

Each assay plate was checked for robustness and reproducibility by calculating the Z'-factor using the following equation:

$$Z' = 1 - \frac{3(\sigma p + \sigma n)}{|\mu p - \mu n|}$$

For the primary screen, positive controls and negative controls were included in columns 1 and 2 respectively. The Z' was found to be on average 0.75, well above the Z'>0.5 which is widely regarded as being suitable for HTS. All 1200 drugs from the Prestwick Chemical Library were screened in duplicate and hits were identified as inhibiting cell growth by ≥75%, as determined by measuring eGFP fluorescence.

Validation of selected hits and MIC determination in liquid media

Drugs selected for further study were purchased from a variety of commercial vendors. Drugs were dissolved into 100% DMSO resulting in a 10 mM stock that was subsequently used to generate a 10-point 3-fold serial dilution which provided a dose response curve with maximum and minimum drug concentration of 500 μM and 0.0254nM, respectively. Data was normalised as described above. The concentration of drug that is required to inhibit cell growth by 99% was calculated by non-linear regression (Gompertz equation for MIC determination, GraphPad Prism).

MIC determination on solid agar.   Selected compounds identified from the secondary MIC screen were further tested for MIC evaluation using solid agar media. Drugs were diluted from a 10mM stock, mixed individually in 2 mLs of molten 7H10 agar and dispensed in square partitioned petri plates. Plates were incubated at 37°C and solid MIC was determined based on absence of colonies.

MIC determination against *M. tuberculosis* H37Rv.   To investigate the effects of repurposed compounds on growth of *M. tuberculosis* H37Rv using an Alamar Blue based MIC assay using the resazurin reagent. This assay was performed in 7H9 medium containing Middlebrook broth and 0.5% glycerol and supplemented with oleic acid, albumin, dextrose, and catalase. Clear- 96-well plates were inoculated with 100 μL of drug diluted with 90 μl of 7H9 medium and 10 μL DMSO. Serial 3-fold dilutions of each drug in 100 μL of 7H9 medium were prepared at various ranges. Growth controls containing no antibiotic and sterility controls without inoculation were also included. 200 μL of sterile deionized water was added to the

outer perimeter wells to prevent evaporation during plate incubation. Plates were incubated plate at 37˚C for 3–4 days. After incubation, the plates were removed and 10 μL of resazurin (0.02% w/v) was added to each well that contained bacteria. Assay plates were reincubated at 37˚C for 24–48 hours and visually assessed for colour development. OD $_{570 \text{ nm}}$ readings were taken to provide further quantitation provide an interpretation of the dose response of the bacterium to repurposed compounds.

HepG2 cytotoxicity assay

Actively growing HepG2 cells were removed from a T-175 tissue culture flask with 5 mL of Eagle's MEM containing 10% FBS/1%NEAA/1% Penicillin and Streptomycin) and mixed with gentle pipetting. Cell cultures were observed to ensure monolayers did not exceed 50% confluence at the time of cell harvest. The cell suspension was added to 250 mL of the same medium at a final density of 6×10^7 cells per mL. This cell suspension (100 μL, typically 6,000 cells per well) was dispensed using multichannel pipette into the wells μClear F-bottom 96-well assay plates (Greiner) pre-loaded with 2-fold serially diluted compounds (final concentration range 250 μM– 0.5 μM). Plates were allowed to incubate at 37˚C at a relative humidity of 80% and 5% CO_2 for 48 hours. After incubation, the plates were allowed to equilibrate at room temperature for 30 mins before 25 μL of CellTitre-Glo (Promega) reagent was added to each well using a multichannel pipette. Plates were left at room temperature for 30 mins before relative luminescence was read using a BMG Labtech POLARstar Omega plate reader. Data was normalised and IC_{50} values determined as concentrations of drug required induce 50% cell viability and was calculated by non-linear regression (GraphPad Prism).

Spontaneous mutant generation

Spontaneous mutants were generated by plating 10^8 cells (*M. smegmatis* and/or BCG) per plate on 7H10 agar with drug concentrations of 2.5x, 5x and 10x the solid MIC values. Plates were incubated at 37˚C for a week or 30 days for *M. smegmatis* and BCG, respectively. Colonies that appeared on plates containing drug at 10X MIC were inoculated into 7H9 re-plated onto 7H9 agar in the presence drugs at 10X MIC in order to confirm resistance. Genomic DNA was isolated for both wild type *M. smegmatis* and BCG strains together with resistant mutants [8,9]. Genomic DNA was submitted to MicrobesNG (https://microbesng.uk/) for whole genome sequencing and SNP variant analysis of the sequence in comparison to the wild type genomic DNA for each strain.

Over-expression of *aroB* and *echA12* in BCG

The production of all oligonucleotide primers (Table 1) and sequencing of generated constructs was performed by Eurofins Genomics, Ebersberg, Germany. Both *echA12* and *aroB* genes were amplified by PCR (Phusion High-Fidelity DNA polymerase; New England Biolabs) from *M. tuberculosis* H37Rv genomic DNA using the oligonucleotide pairs shown in Table 1. The resulting fragments were cloned into the mycobacterial shuttle vector pVV16 by using *NdeI* and *HindIII* restriction sites (FastDigest restriction endonucleases and T4 DNA ligase, Fermentas). All constructs were verified by DNA sequencing. pVV16-*aroB*, pVV16-*echA12* and empty pVV16 (control) were electroporated into *M. bovis* BCG Pasteur strain.

Table 1. Primers used for the construction of pVV16-*echA12* and pVV16-*aroB*.

Primer	Sequence (5'→3')[a]
echA12 _forward	GATCGATCCATATGGCTGTGCCCCACCGCTGC
*echA12*_reverse	GATCGATCAAGCTTCGTGTCATCGGTGAACACCGG
*aroB*_forward	GATCGATCCATATGATGACCGATATCGGCGCACCC
*aroB*_reverse	GATCGATCAAGCTTTGGGGCGCAAACTCCGGCGTA

[a] restriction sites used for cloning are underlined (*NdeI* and *HindIII*).

Results

Primary screening of the Prestwick Chemical Library against *M. smegmatis* and BCG

To identify which of the 1200 FDA approved drugs in the Prestwick Chemical Library inhibit the growth of mycobacteria, a medium throughput fluorescence screen was used to measure GFP expression in strains of both *M. smegmatis* and BCG (GFP microplate assay [GFPMA]) [10]. *M. smegmatis*_pSMT3_eGFP and BCG_pSMT3_eGFP were cultured in 96-well plates in the presence of 20 μM compound from the Prestwick Chemical Library. GFP fluorescence was measured at specified time points and data was normalized against both positive and negative controls to produce a scatter graph of the survival percentages (Fig 1). In order to assess the reproducibility and robustness of the GFPMA HTS, we calculated Z'factor values for each of the assay plates used to screen the 1200 compounds of the Prestwick Chemical Library against both *M. smegmatis*_pSMT3_eGFP and BCG_pSMT3_eGFP. The Z' values of the primary screen against *M. smegmatis* vary between 0.4 and 0.9 across each of the assay plates used in the screen (S1 Fig). In case of the primary screen for BCG, the Z'values are consistent between 0.8 and 0.9 across all assay plates (S1 Fig). However, since all assay plates used in the experiment derived Z' values $\geq$ 0.4, all data generated was deemed suitable for further processing [11].

In order to understand the variability in the data and significance of the hits identified from the scatter plot (Fig 1), we analysed the variance of data both between and across replicate experiments carried out using *M. smegmatis* and BCG. The overall coefficient of correlation (r^2) values for replicate assays were calculated to be 0.63 and to 0.89 for *M. smegmatis*_pSMT3_eGFP and BCG_pSMT3_eGFP, respectively (Fig 2). This indicates increased variance in the data for assays conducted with *M. smegmatis* compared to screens performed using BCG. We analysed the frequency distribution of data both within and across each primary screen using *M. smegmatis* and BCG (Fig 3). For *M. smegmatis*, we observed that 31.5% of the compounds screened in the library induced $\leq$ 75% survival of bacterial cell growth in the primary screen (Fig 3). For BCG, 21% of the library induced $\leq$ 75% survival of bacterial cell growth in the primary screen (Fig 3). We applied a minimum cut-off of $\leq$25% bacterial cell survival at 20 μM compound, as a parameter that defined an antimycobacterial hit that would be further investigated in downstream experiments (Fig 1). In this regard, we observed an almost identical hit rate of 6.9% and 6.8% for compounds inducing $\leq$ 25% survival for *M. smegmatis* and BCG, respectively (Fig 3).

The initial screen against *M. smegmatis* generated 83 hits which inhibited the survival of this fast-growing species of mycobacterium below 25% (Fig 1A). The screen against the slower growing mycobacterial strain BCG revealed 81 hits (Fig 1A) which inhibited the growth of the bacteria below 25% (Fig 1B). Categorisation of these hits (<25% survival) into pharmacological

A

B
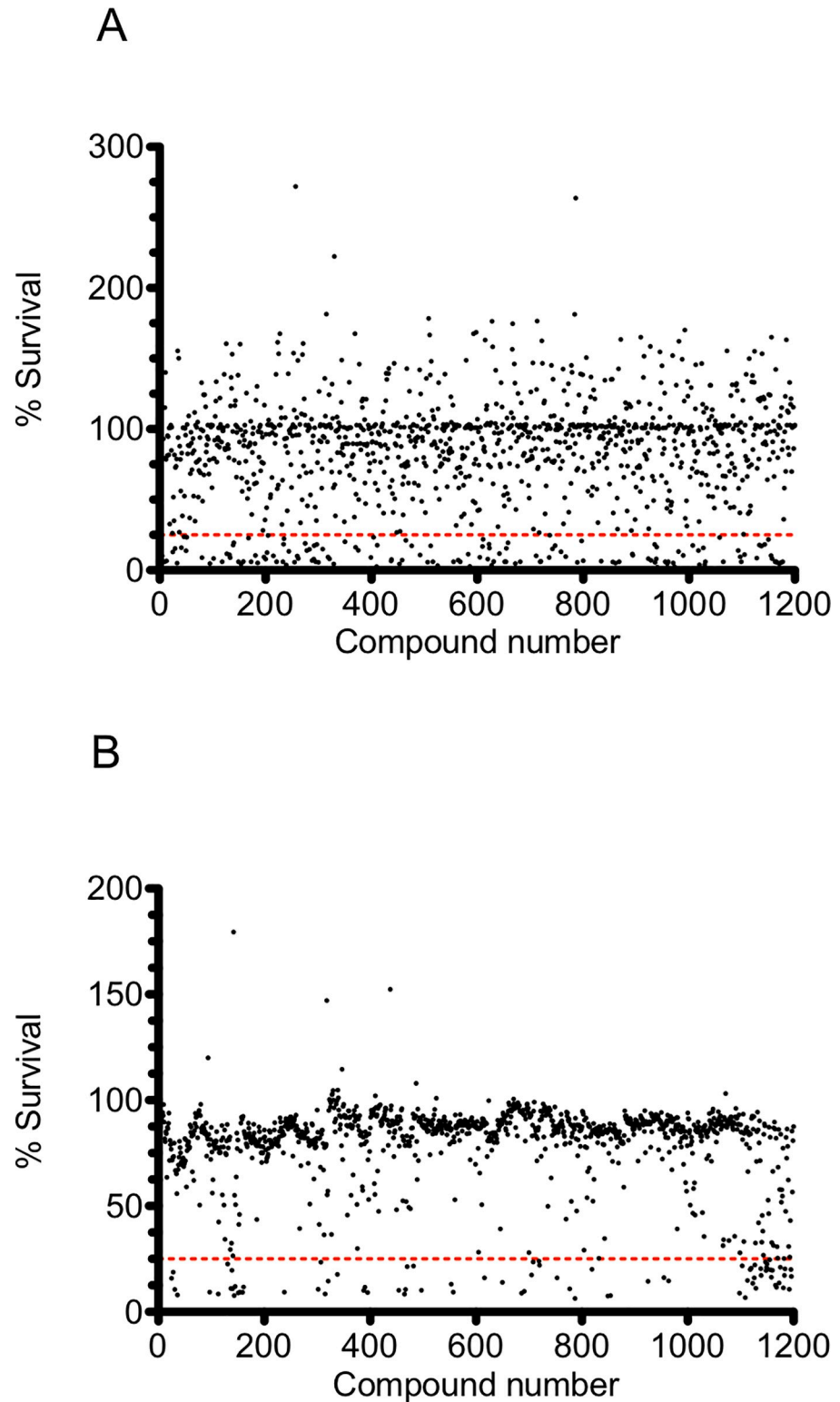
Fig 1. Primary screening of the Prestwick Chemical Library compounds against *M. smegmatis* (A) and BCG (B) using a GFPMA assay. GFP measurements were recorded after a defined period of incubation of mycobacteria in the presence of 20 μM compound from the Prestwick Chemical Library. Data was normalised to control wells and is expressed as mean % survival from n = 2 biological replicate experiments. The red dashed line depicts <25% cell survival as determined by residual GFP fluorescence.

A

B

C

Fig 2. Correlation analysis of the primary screen against the Prestwick Chemical Library. Scatter graphs representing correlation analysis of the cumulative data of the percentage survivals between n = 2 biological replicate experiments (run A and B) dur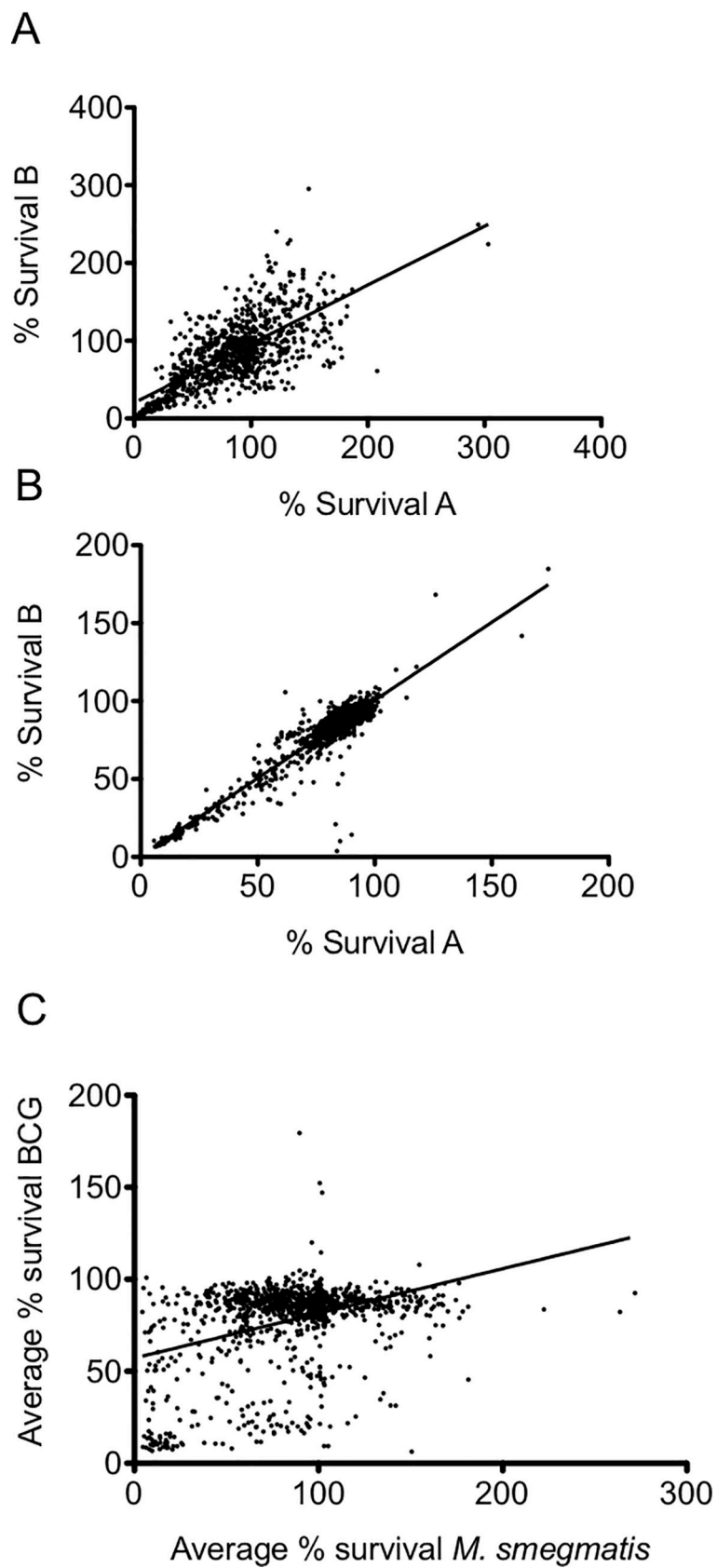ing the primary screen of the Prestwick Chemical Library against *M. smegmatis* (A) and BCG (B). The average of run A and B data sets from both *M. smegmatis* (A) and BCG were plotted against each other (C).

groups reveals that an almost equal number of fluoroquinolones, macrolides, polyketide antibiotics, antimycobacterial drugs, and antiseptics display inhibitory activity against both *M. smegmatis* and BCG whilst the aminoglycosides displayed more inhibitory activity towards *M. smegmatis* compared to BCG (Fig 4). Other notable classes of drugs that inhibit the growth of both *M. smegmatis* and BCG include the amphenicols, glycopeptides and non-ribosomal peptide antibiotics, antihistamines, acetylcholine esterase inhibitors, antiemetic, antimalarial, antiprotozoal and surfactants (Fig 4). Notable species-specific inhibitors affecting only *M. smegmatis* were also identified belonging to antiestrogen, antiarrhythmic and antipsychotic drugs (Fig 4). For BCG, it appears that the cephalosporin antibiotics are only able to inhibit the slower growing mycobacterial species and do not affect the faster growing saprophytic organism *M. smegmatis*. Other significant drug classes that only inhibit BCG include anticancer agents, antidiabetics, anticonvulsants and angiotensin antagonists (Fig 4).

All hits from the primary screen (displaying <25% survival) were filtered to remove all known antimycobacterial drugs (isoniazid, rifampicin, ethambutol, streptomycin, pyrazinamide [active only for BCG]), and a significant number of other antimicrobial agents [7].The remaining drugs were then clustered into one of three groups based upon their inhibitory
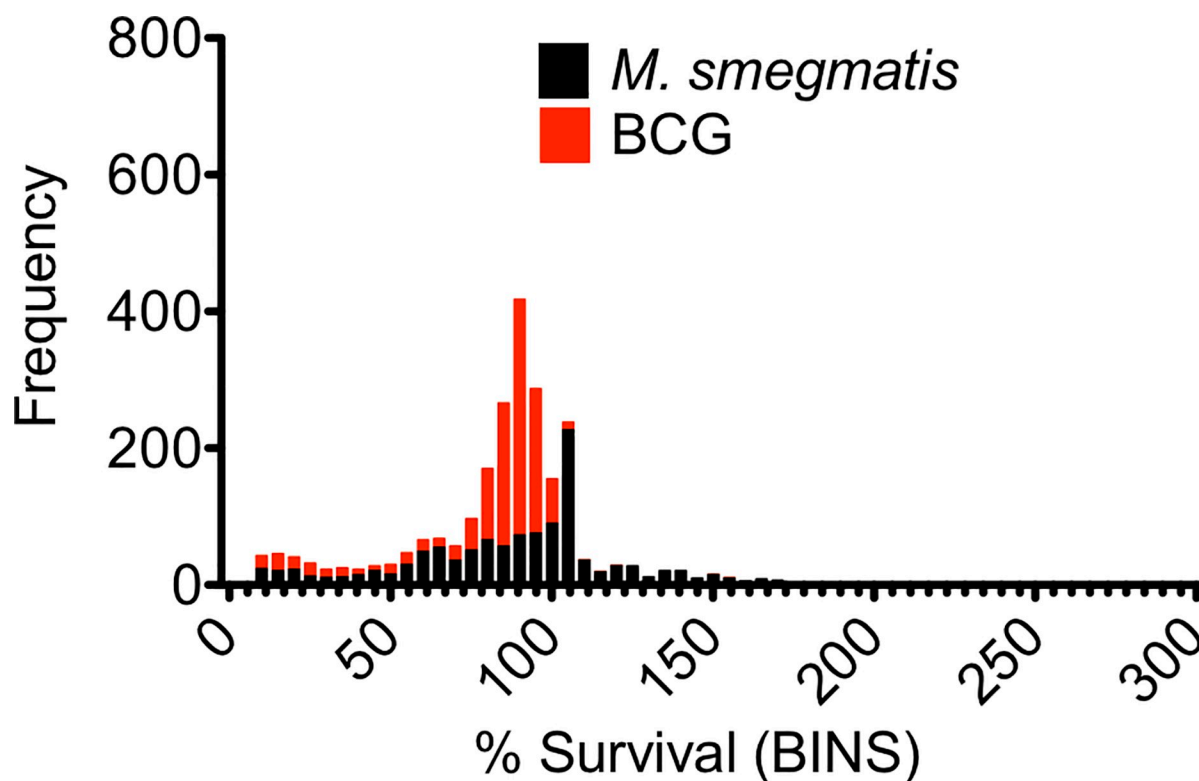
Fig 3. A comparative frequency distribution of the primary screening against the Prestwick Chemical Library. Each bar represents the comparative frequency distribution primary screening data (averaged) for *M. smegmatis* (black) and BCG (red). % survival data for was 'binned' into groups of 5%.
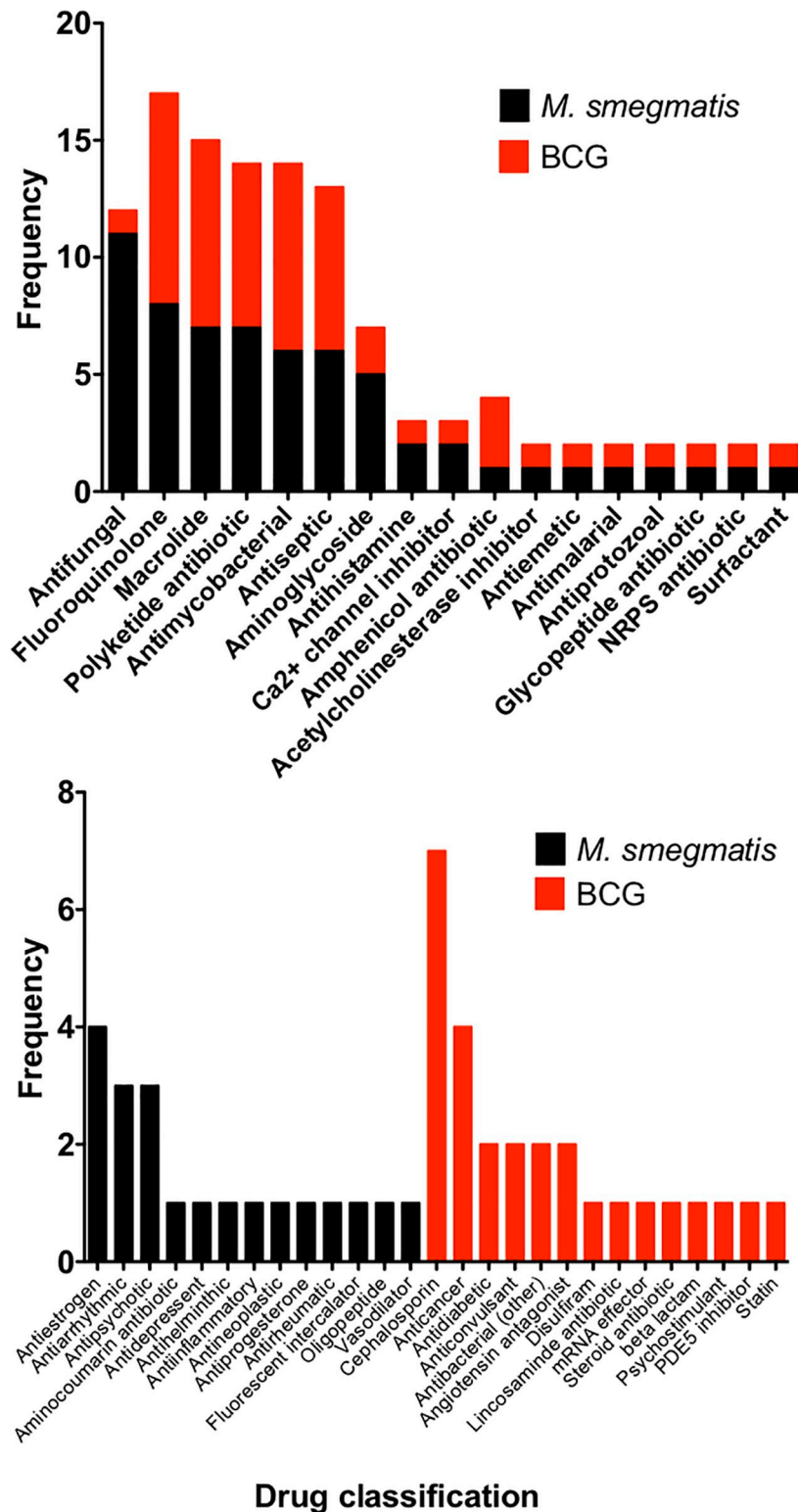
Fig 4. Comparison of the hits emerging from the primary screen active against both *M. smegmatis* and BCG.
Drugs were grouped into drug classifications and are plotted as frequency of hits against either *M. smegmatis* or BCG.

activity against either fast-growing (*M. smegmatis*) or slow-growing (BCG) strains of mycobacteria, or those showing overlapping activity. Each cluster of drugs was further ranked and given a priority score that was based on the apparent potency of the drug and potential novelty of its mode of action from literature-based searches.

Secondary screening and hit confirmation against *M. smegmatis*

Minimal Inhibitory Concentrations (MIC) were determined using the standardized broth dilution method and then subsequently measured on solid medium in order to ascertain the concentration required to generate resistant mutants (S2 Fig). Among the drugs tested against *M. smegmatis*, the most potent was meclocycline sulfosalicylate with a liquid and solid MIC of 0.10 μM and 0.2 μM, respectively (Table 2). Auranofin also displayed a relatively low solid MIC of 6.0 μM although this was 12-fold higher than its liquid MIC values (0.51 μM). Other drugs tested for MIC determination were alexidine and chlorhexidine which both exhibited relatively low MIC values of 6.15 μM and 1.98 μM, both of which are used as antimicrobials in dentistry [12]. The estrogen receptor modulating drugs clomiphene citrate, raloxifen, toremifene and tamoxifen citrate [13–14] displayed liquid MIC values ranging from 9.03μM to 26.64 μM (Table 2). GBR12909 (Vanoxerine), a dopamine transport inhibitor [15], displayed a liquid MIC of 18.6 μM (Table 2). Two of the drugs tested against *M. smegmatis*, auranofin and ebselen, displayed MIC values of 0.51 μM and 10.3 μM respectively while other drugs which were initially identified as hits from the primary screen (fendiline hydrochloride, sulocitidil, apomorphine, nisoldipine, sertraline and fluspirilene) displayed relatively high MIC values that ranged from 77 μM to 827.5 μM (Table 2). Some drugs initially examined were excluded from further solid media MIC testing (alexidine dihydrochloride, ebselen and fluspirilene). Fluspirelene displayed a relatively high liquid MIC and alexidine dihydrochloride was discounted for further study due to its structural and functional similarity to chlorhexidine.

Table 2. MIC determination of selected drugs shortlisted as hits from the whole cell screen of the Prestwick Chemical Library against *M. smegmatis*.

Shortlisted Drugs (*M. smegmatis*)	Liquid MIC (μM)	Solid MIC (μM)
Meclocyline sulfosalicylate*	0.10	0.20
Auranofin	0.51	6.0
Chlorhexidine	1.95	16.0
Alexidine	6.15	N/T
Clomiphene citrate*	9.03	37.5
Ebselen	10.3	N/T
Raloxifene	25.7	312.5
Toremifene	23.76	62.5
Tamoxifen citrate*	26.48	31.25
GBR 12909*	18.6	62.5
Fendiline hydrochloride	77.57	15.63
Sulocitidil	87.22	625
Apomorphine	241.7	625
Nisoldipine	396.2	100
Sertraline	526.7	90
Fluspirilene	827.5	N/T

MICs were determined using both liquid and solid growth mediums. (N/T)—not tested.

*Selected for generation of drug resistant mutants. Experiments were carried out at least three independent times and representative data are shown.

Further investigation of ebselen ceased due to mode of action deconvolution that has been previously determined elsewhere [16]. Ebselen is an organoselenium compound approved by the FDA with a well-known pharmacological profile and is currently being investigated for clinical use in the treatment of bipolar disorders and strokes. Previous studies have shown that ebselen displays antimycobacterial properties and is also effective against multidrug resistant *Staphylococcus aureus* (MRSA) [2]. In *M. tuberculosis*, ebselen acts by covalently binding to an active site cysteine residue in antigen 85. Antigen 85 is a complex of secreted proteins (Ag85A, Ag85B and Ag85C) which play an important role in the synthesis of trehalose dimycolates (TDM) and mycolylarabinogalactan (mAG) [16].

Secondary screening and hit confirmation against BCG

MIC studies of the compounds listed in Table 3 revealed thonzonium bromide as having the lowest MIC value of 0.16μM. Thonzonium bromide is a quaternary ammonium monocationic compound which is used as a surfactant and a detergent and has been known to disrupt ATP dependant proton transport in vacuolar membranes along with alexidine dihydrochloride, which are responsible for pH regulation in yeast and *Candida albicans* causing growth defects [17]. Florfenicol, a fluorinated analogue of thiamphenicol with broad spectrum activity against Gram negative bacteria and strains resistant to chloramphenicol and thiamphenicol [18], displayed broth and solid MIC values of 0.67μM and 6 μM against BCG, respectively (Table 3). Florfenicol is known to influence the microbiota of the intestine reducing the amount of uncultured bacterial species similar to *Corynebacterium* and *Mycobacterium* [19]. Josamycin, a 16-membered macrolide with inhibitory activity against both Gram negative and Gram positive bacteria [20], displayed potent activity against BCG with an MIC of 0.1μM (Table 3). Interestingly, we identified three antihistamines as having inhibitory activity against BCG. Astemizole had the lowest MIC value of 17.8μM within this group followed by tripelennamine, with an MIC of 41.9μM and olopatadine with the highest MIC value of 202.3 μM in (Table 3). Astemizole (used for general allergies, asthma and rhinitis), tripelennamine (hay fever and

Table 3. MIC determination of selected drugs shortlisted as hits from the whole cell screen of the Prestwick Chemical Library against BCG.

Shortlisted Drugs (BCG)	Liquid MIC (μM)	Solid MIC (μM)
Thonzonium *	0.16	5
Florfenciol *	0.67	6
Pentamidine *	3.23	50
Astemizole	17.78	50
Pinaverium	28.29	50
Josamycin	0.10	>100
GBR 12909 *	20.5	28.2
Tripelennamine *	41.9	100
Rosiglitazone	43.15	≥ 1500
Glipizide	191.10	≥ 500
Olopatadine	202.30	≥ 500
Granisteron	210.60	≥ 500
Phenteramine	375.00	N/T

MICs were determined using both liquid and solid growth mediums. (N/T)—not tested.

*Selected for generation of drug resistant mutants. Experiments were carried out at least three independent times and representative data are shown.

rhinitis) and olopatadine (allergic conjunctivitis) are mildly anti-cholinergic and act as H1 receptor antagonists [21–24]. Of the antidiabetic drugs displaying activity towards BCG, glipizide and rosiglitazone have an MIC value of 191.1 μM and 43.15 μM, respectively (Table 3). Glipizide is a second-generation sulfonylurea drug that is prescribed for hypoglycaemia in type II diabetes and is known to act by stimulating insulin production and correcting cellular lesions which occur during diabetes mellitus [25–26]. Rosiglitazone, on the other hand, functions by activating peroxisome proliferator activated receptors in adipocytes and sensitising them to insulin [27]. Pinaverium, that inhibits L-type calcium channels arresting influx of the Ca^{2+} [28], had an MIC of 28.3μM. Two other drugs which displayed relatively high MIC values were granisetron and phentermine (Table 3). Granisetron, an antiemetic drug which is an agonist to the 5-hydroxytryptamine-3 receptor, stimulates the vagus nerve responsible for reflex motility response [29], had an MIC value of 210.6μM. Phentermine, which has been prescribed as an appetite suppressant to control obesity and acts as an agonist to the human TAAR1 (Trace Amine Associate Receptor 1) [30], displayed an MIC of 375.00 μM and was not tested further due to the high concentrations required for inhibitory activity. These drugs were then further tested to establish MICs on solid media in order to determine accurate concentrations to generate spontaneous resistant mutants for mode of action studies. We observed that, upon solid agar MIC testing against BCG, the general trend was that the drugs displayed 5 to 100-fold higher MIC values when compared to MIC values obtained by broth dilution method. For some of the drugs this was attributed to low solubility in solid media as many precipitated during the cooling of the agar medium. Glipizide, olopatadine and granisetron yielded solid MIC values greater than 0.5 mM; these drugs precipitated out at higher concentrations and appeared to show no noticeable inhibitory activity against BCG (S3 Fig). Rosiglitazone displayed the highest MIC value at approximately 1.5 mM. Thonzonium and florfenicol had a 5-fold increase in their solid MIC values but were still around 5μM and effectively inhibited the growth of BCG on solid agar (Table 3). Pentamidine, astemizole and pinaverium had solid MIC values of around 0.05 mM while there was a 2-fold increase in the MIC value for tripelennamine (compared to its liquid MIC) of 0.1 mM (Table 3).

All compounds listed in Tables 2 and 3 were tested in an Alamar Blue assay against *M. tuberculosis* (S4 Fig) and the drugs that displayed any notable anti-TB activity are listed in Table 4. Both ebselen and auranofin displayed MICs of 18.51 μM and 0.27 μM, which are in close agreement with previously published values [16,31]. In addition, the estrogen receptor

Table 4. MIC determination of selected drugs against *M. tuberculosis* H37Rv.

Shortlisted Drugs (*M. tuberculosis*)	Liquid MIC (μM)	IC$_{50}$ (μM) HepG2 cells
Ebselen	18.51	45
Clomiphene	7.59	35
GBR 12909	26.64	55
Raloxifen	22.10	20
Tamoxifen	≥ 100	30
Auranofin	0.27	3
Pentamidine	10.51	3.5
Tripelennamine	49.3	>250
Florfenicol	25.4	>250

MICs were determined in liquid growth media using the Alamar Blue assay (S4 Fig). Cytotoxicity IC$_{50}$ values against HepG2 cell were determined using the CellTitre-Glo (Promega) assay. Experiments were carried out at least three independent times and representative data are shown.

modulating drugs clomiphene and raloxifene inhibited the growth of *M. tuberculosis* H37Rv with MICs of 7.59 μM and 22.10 μM, respectively (we were unable to accurately determine the MIC for Tamoxifen) (Table 4). Finally, GBR12909 (used in the clinic to treat cocaine addiction), inhibited the growth of *M. tuberculosis* with an MIC of 26.64 μM. It is interesting to note clear differences in MIC values obtained from either *M. smegmatis* and/or BCG (Table 2 and Table 3) when compared to those obtained in *M. tuberculosis* (Table 4), which can be partially attributed to differences in cell physiology and efflux pump expression [7].

Generation of spontaneous resistant mutants to determine mode of action

We attempted to generate spontaneous resistant mutants in both *M. smegmatis* and BCG against a selection of drugs identified in Tables 2 and 3, respectively. However, we were only able to obtain drug-resistant isolates for meclocyline sulfosalicylate, tamoxifen citrate and GBR12909 in *M. smegmatis* (Table 5) and florfenicol, pentamidine and tripelennamine in BCG (Table 6). Analysis of the *M. smegmatis* meclocyline sulfosalicylate mutant revealed a synonymous single nucleotide polymorphism (SNPs) mutation in the gene MSMEG_3619 (*Mtb* ortholog Rv1856c), a probable oxidoreductase deemed non-essential by the Himar-I based transposon mutagenesis [21], but also showing importance as having a growth advantage which results in an improvement in fitness when disrupted [32]. A single SNP (P122S) was also observed in MSMEG_5249 (*Mtb* ortholog Rv1093) *glyA1* which is a serine hydroxymethyltransferase with possible roles of glycine to serine inter-conversion and the generation of 5, 10-methenetetrahydrofolate which plays an important role in providing precursors for cellular redox balancing, methylation reactions and a role in thymidylate biosynthesis (Table 5). *GlyA1* is also thought to be an essential gene [32,33] and it has also been identified as one of the proteins which undergoes PUPylation (Ubiquitinylation by prokaryotic ubiquitin protein) in mycobacteria [34]. The *M. smegmatis* tamoxifen citrate resistant mutant exhibited a frame shift mutation in the gene MSMEG_6431 (*Mtb* ortholog Rv3849) *espR* which encodes for a protein involved in transcriptional regulation of the three genes Rv3136c-Rv3614c required for the ESX-1 system (Table 5). EspR binds to the promotor region and regulates

Table 5. Mode of action determination of drugs inhibiting *M. smegmatis* through whole genome sequencing and variant analysis of spontaneous resistant mutants.

Drug Name (*M. smegmatis* hits)	Mutated Genes	Rv Number	Positions	Amino acid substitutions	Probable function
Meclocycline	MSMEG_3619	Rv1856c	A/G		Short chain dehydrogenase/ oxidoreductase
Meclocycline	MSMEG_5249 (*glyA1*)	Rv1093	Ccg/Tcg	P122S	Serine hydroxymethyltransferase
Tamoxifen	MSMEG_6431 (*espR*)	Rv3849	ttc/ (Frame shift)	F24	Conserved hypothetical protein
GBR12909	MSMEG_3033 (*aroB*)	Rv2538c	Ggg/Agg	G282R	Involved at the second step in the biosynthesis of chorismate within the biosynthesis of aromatic amino acids (the shikimate pathway) [catalytic activity: 7-phospho-3-deoxy-arabino-heptulosonate = 3-dehydroquinate + orthophosphate].
GBR12909	MSMEG_3033 (*aroB*)	Rv2538c	gGc/gAc	G284D	
GBR12909	MSMEG_3033 (*aroB*)	Rv2538c	Tgc.GTtgc (Frame shift)	C356V	
GBR12909	MSMEG_3033 (*aroB*)	Rv2538c	cTa/cCa	L363P	

The table represents the single nucleotide polymorphisms obtained through whole genome sequencing of the spontaneous resistant mutants raised compared against drug sensitive *M. smegmatis*.

https://doi.org/10.1371/journal.pone.0213713.t005

ESX-1, therefore controlling virulence of mycobacteria [35]. Spontaneous resistant mutants raised against GBR12909 in *M. smegmatis* produced consistent multiple mutations in MSMEG_3033 (*aroB*) (Table 5). *AroB* is predicted to be an essential gene as studied *in M. tuberculosis* [32,33] and it encodes for 3-dehydroquinote synthase, which is one of several enzymes participating in the shikimate biosynthetic pathway [36]. AroB is a homomeric enzyme, is the second enzyme in the shikimate biosynthetic pathway and is present in various bacterial species such as *Corynebacterium glutamicum*, *Escherichia coli*, *Bacillus subtilis* and other fungi, plants and apicomplexan parasites [37–39]. AroB makes for an important target due to its essentiality in *M. tuberculosis* and absence of this biochemical pathway in mammals [32,33,37]. To further support the evidence that AroB is the target of GBR12909, AroB was over-expressed in BCG using the expression plasmid pVV16, which constitutively expresses *aroB* under the control of the *hsp60* promoter, and the MIC of GBR12909 was reassessed. In the absence of AroB over-expression (pVV16 empty vector control), the MIC of GBR12909 unchanged with that of wild-type BCG (Fig 5 and Table 3). However, upon over-expression of AroB, the MIC of GBR12909 increased from 20.5 µM to > 50 µM (Fig 5). These results further substantiate AroB as the target of GBR12909 as over-expression of AroB provides additional inhibitor protein target, thus allowing the bacteria to survive at elevated drug concentrations.

Spontaneous resistant mutants were raised against florfenicol in BCG, and whole genome sequencing revealed a point mutation in BCG_1533 (*echA12*) gene which encodes for a putative enoyl CoA hydratase (Table 6). EchA12 has been shown to be membrane localized within the mycobacterial cell membrane [40], however the gene was not found to be essential through Himar-I based transposon mutagenesis [32,33]. It has been suggested that EchA12 is involved in lipid membrane metabolism and is found to co-localise with thioredoxine A [40] and CtpD, which is an ATPase involved with the metalation of proteins secreted during redox stress [41]. Again, to provide further evidence that EchA12 is targeted by florfenicol, we over-expressed

Table 6. Mode of action determination of drugs inhibiting BCG through whole genome sequencing and variant analysis of spontaneous resistant mutants.

Drug Name (BCG hits)	Mutated Genes	Rv Number	Positions	Amino acid substitutions	Probable function
Florfenicol	BCG_1533 (EchA12)	Rv1472	Gga/Aga	G239R	Possible enoyl-CoA hydratase echA12 [*Mycobacterium bovis* BCG str. Pasteur 1173P2]
Florfenicol	BCG_3158 (PPE50)	Rv3135	gGc/gAc	G251D	PPE family protein
Florfenicol	BCG_3508 (rpsI)	Rv3442c	Ccc/Gcc	P17A	Probable 30S ribosomal protein S9 RPSI
Florfenicol	BCG_3755c (glpK)	Rv3696c	gTc/gCc	V271A	Probable glycerol kinase GlpK (ATP glycerol 3-phosphotransferase)
Pentamidine	BCG_0763	Rv0713	aTt/aCt	I274T	Probable conserved transmembrane protein [*Mycobacterium bovis* BCG str. Pasteur 1173P2]
Pentamidine	BCG_0763	Rv0713	gCg/gTg	A281V	
Pentamidine	BCG_1609 (mmpL6)	Rv1557	Gcc/Acc	A31T	Probable conserved transmembrane protein
Pentamidine	BCG_3755c (glpK)	Rv3696c	gTc/gCc	V271A	Probable glycerol kinase GlpK (ATP glycerol 3-phosphotransferase)
Trippelennamine	promoter region of gene BCG_3090	Rv3065	Upstream gene BCG 3089c (Rv 1904)		Multi-drug transport integral membrane protein (efflux pump)
	glpK	Rv3696c	gTc/gCc	V271A	Probable glycerol kinase GlpK (ATP glycerol 3-phosphotransferase)

The table represents the single nucleotide polymorphisms obtained through whole genome sequencing of the spontaneous resistant mutants raised compared against drug sensitive BCG.
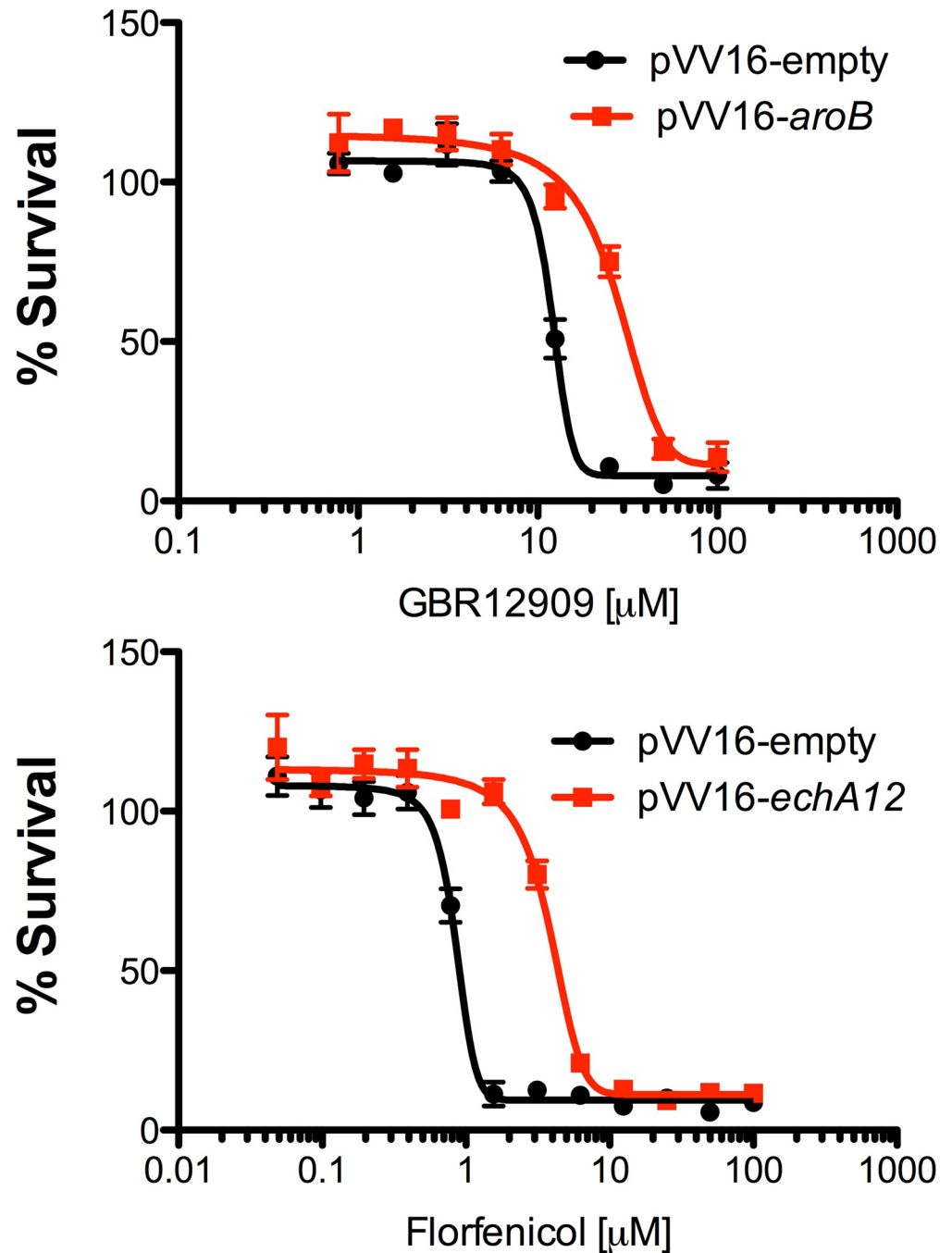
https://doi.org/10.1371/journal.pone.0213713.t006

Fig 5. Effect on the MIC of GBR12909 and florfenicol on the over-expression of AroB and EchA12 in BCG. The over-expression constructs pVV16-*aroB*, pVV16-*echA12* and empty pVV16 (control) were electroporated into BCG and the MICs GBR12909 and florfenicol evaluated. The data shows a mean of three replicates and error bars represent the standard deviation.

https://doi.org/10.1371/journal.pone.0213713.g005

EchA12 in BCG. In the absence of EchA12 over-expression, the MIC of florfenicol remained unchanged with that of wild-type BCG (Fig 5 and Table 3). However, upon over-expression of EchA12, the MIC of florfenicol increased from 0.7 μM to > 12 μM (Fig 5) highlighting target engagement of florfenicol with EchA12 as one of its putative targets in mycobacteria. Three

additional point mutations were also observed in the florfenicol resistant mutant. A single gua-
nine to adenine point mutation in the gene BCG_3185 (PPE50) which encodes for a protein
belonging to the PPE family, generates a G251D mutation. Florfenicol is a fluorinated form of
thiamphenicol which belongs to the amphenicol family of antibiotics, whose mode of action is
through binding to the 23S rRNA of the 50S ribosomal unit [42]. BCG_3508 (*rpsI*) encodes for
a probable 30S ribosomal protein and contains a P17A mutation in the florfenicol mutant
(Table 6), which suggests that florfenicol could hit multiple targets in mycobacteria. Finally,
we also observed a V271A point mutation in BCG_3755c, which encodes for a glycerol kinase
(GlpK), which catalyses the rate limiting step in glycerol metabolism of converting glycerol to
glycerol-3-phosphate [43,44]. Mutations in *glpK*, have previously been observed when generat-
ing resistant mutants to drugs in an attempt to deconvolute their mode of action [45,46]. In
our investigation of pentamidine activity, we identified an identical mutation in *glpK*, two sep-
arate non-synonymous SNPs in BCG_0763, which encodes for putative membrane protein
with a domain of unknown function, and a single SNP in BCG_1609, which encodes for
mmpl6 (Table 6). Mycobacterial membrane protein large (MmpL) are membrane proteins
involved in shuttling lipid components across the plasma membrane and have been known to
play an important role in drug resistance mechanisms, membrane physiology and virulence of
the bacterium [47]. The tripelennamine mutant had a single point mutation in the promoter
region of BCG_3090, a multi-drug transport integral membrane protein (*mmr*) (Table 6),
which is a known efflux pump involved in drug resistance with high susceptibility to quater-
nary compounds [48]. This suggests that exposure to tripelennamine might induce a mutation
that causes increased overexpression of Mmr which could alter the ability of the bacterium to
efflux drugs.

Discussion

Screening compounds against *M. smegmatis* has a distinct advantage over the slower growing
BCG strain in terms of its shorter generation time, thus expediting the generation of screening
data and turnaround of results. However, using *M. smegmatis* as a screening organism is less
efficient in determining antitubercular compounds than BCG. It was observed during a screen
of the LOPAC library against *M. tuberculosis*, *M. smegmatis* and BCG that 50% of the drugs
inhibiting *M. tuberculosis* were not identified in *M. smegmatis* while it was only 21% of the
drugs that were not identified in BCG. In addition, it was observed that 30% of proteins *in M.
tuberculosis* do not have conserved orthologs in *M. smegmatis* [7]. Despite this fact, bedaqui-
line, the most recent drug given FDA approval for the treatment of MDR-TB, was initially dis-
covered through a whole cell screen assay against *M. smegmatis* [49], which makes the case for
not excluding *M. smegmatis* as a model organisms for antitubercular drug screening.

Although genetically similar, there are a number of physiological variations between *M.
tuberculosis* and BCG which have been attributed to the differential expression of around 6%
of genes across their respective genomes. During the exponential growth of both organisms,
major variations were observed for genes involved in cell wall processes, intermediary metabo-
lism and respiration and hypothetical proteins [50]. In addition, in *M. tuberculosis* the PE/PPE
genes were found to be highly expressed whereas in BCG, there are a higher number of tran-
scriptional regulators that are overexpressed during exponential growth. These variations in
gene expression profiles of mycobacteria partly explain why different classes of drugs differen-
tially inhibit each strain utilised during screening experiments (Fig 4).

Target deconvolution of hits that emerge from whole cell screening efforts has long been
the bottleneck of phenotypic-based drug discovery; often huge investment of time and
resource is required to identify the precise molecular target of active compounds [51].

Interestingly, in the case of early stage drug discovery in *M. tuberculosis*, there seems to be an apparent trend whereby inhibitors of cell growth/viability obtained through phenotypic screening efforts tend to inhibit membrane targets such as DprE1, MmpL3, QcrB and Pks13 [52]. This relatively high probability of hits inhibiting membrane targets could, in part, be due to the hydrophobicity of the inhibitors screened in libraries against mycobacteria [52,53]. For instance, several drugs from the Prestwick Chemical Library that inhibit the growth of myco-bacteria have an average clogP value of 5.7 [52]. Hydrophobic drugs have a tendency to enter into the lipid layers of the mycobacterial cell envelope and then move laterally through the membrane due to their inability to cross the plasma membrane into the cytoplasm. While tra-versing the bilayer, these hydrophobic compounds interact with membrane proteins thereby increasing the probability of these drugs inhibiting such targets. In doing so, such hydrophobic inhibitors drive spontaneous resistant mutants in membrane targets during mode of action studies [52]. Alexidine dihydrochloride and thonzonium bromide were amongst the hits observed in this study that have uncoupling properties and might generated a membrane pro-tein mutation [17]. In this study, screening the Prestwick Chemical Library also identified inhibitors such as calcium channel blockers, antihistamines, antifungal azoles and, unsurpris-ingly, a variety of anti-infectives (Fig 4). Calcium channel inhibitors are generally small hydro-phobic molecules which have the ability to enter the phospholipid bilayer and can diffuse through the membrane inhibiting metabolic functions due to interactions with proteins and boundary lipids [54]. Antifungal azoles, which have been shown to elicit inhibitory activity against mycobacteria, act by targeting the CYP121 and CYP130 cytochrome P450 systems [55]. Arguably, the most interesting hits emerging from this study are florfenicol, GBR12909 (vanoxerine) and pentamidine as (to date) there is little information regarding their anti-mycobacterial activity. Indeed, our SNP analysis spontaneous resistant mutants raised to these compounds (Tables 4 and 5) and over-expression of AroB and EchA12 (Fig 5) marks the beginning of an extensive target deconvolution effort currently underway in our laboratory. Overall, our screening of the Prestwick Chemical Library and preliminary analysis of unique emerging hits, provides new impetus to explore drug repurposing as a feasible and efficient way of mining for new anti-mycobacterial drugs.

Supporting information

S1 Fig. Z' factor analysis of each assay plate used in the primary screen of the Prestwick Chemical Library against *M. smegmatis* (smeg) and BCG.
(PDF)

S2 Fig. Solid MIC testing of preliminary hits from the Prestwick Chemical Library *M. smegmatis.* The solid MIC testing was performed against a. Sulocitidil, b. Auranofin, c. Raloxi-fen, d. Clomiphene citrate, e. Chlorhexidine, f. Fendiline hydrochloride, g. Tamoxifen citrate, h. Meclocyline sulfosalicylate, i. GBR12909, j. Nisoldipine, k. Sertraline, l. Toremifene, m. Apo-morphine in the presence of a negative and positive control.
(PDF)

S3 Fig. Solid MIC testing of preliminary hits from the Prestwick Chemical Library against BCG. The solid MIC testing was done against a. Rosiglitazone, b. Pinaverium, c. Astemizole, d. Olopatadine, e. Glipizide, f. Tripelennamine, g. Pentamidine, h. Thonzonium, i. Florfenicol, j. Josamycin in the presence of a negative and positive control.
(PDF)

S4 Fig. Effect on growth of selected hits from the Prestwick Chemical Library against *M. tuberculosis* H37Rv. The data shows a mean of three replicates. The OD values are derived

from subtracting the OD from the test well which had been inoculated with *M. tuberculosis* from a blank well which had not been inoculated with bacteria. The error bars represent the standard error of the mean.
(PDF)

Acknowledgments

Author Contributions

Conceptualization: Panchali Kanvatirth, Luke J. Alderwick.

Data curation: Rose E. Jeeves, Luke J. Alderwick.

Formal analysis: Panchali Kanvatirth, Rose E. Jeeves, Joanna Bacon, Luke J. Alderwick.

Funding acquisition: Gurdyal S. Besra, Luke J. Alderwick.

Investigation: Panchali Kanvatirth, Rose E. Jeeves, Luke J. Alderwick.

Methodology: Luke J. Alderwick.

Project administration: Luke J. Alderwick.

Resources: Joanna Bacon, Gurdyal S. Besra, Luke J. Alderwick.

Supervision: Gurdyal S. Besra, Luke J. Alderwick.

Validation: Joanna Bacon.

Writing – original draft: Panchali Kanvatirth, Rose E. Jeeves, Luke J. Alderwick.

Writing – review & editing: Luke J. Alderwick.

References

1. WHO | TB emergency declaration [Internet]. WHO. [cited 2018 Jun 26]. Available from: http://www.who.int/tb/features_archive/tb_emergency_declaration/en/

2. Thangamani S, Younis W, Seleem MN. Repurposing Clinical Molecule Ebselen to Combat Drug Resistant Pathogens. PLoS ONE. 2015; 10(7):e0133877. https://doi.org/10.1371/journal.pone.0133877 PMID: 26222252

3. Maitra A, Bates S, Shaik M, Evangelopoulos D, Abubakar I, McHugh TD, et al. Repurposing drugs for treatment of tuberculosis: a role for non-steroidal anti-inflammatory drugs. Br Med Bull. 2016 Jun 1; 118 (1):138–48. https://doi.org/10.1093/bmb/ldw019 PMID: 27151954

4. Ramón-García S, González del Río R, Villarejo AS, Sweet GD, Cunningham F, Barros D, et al. Repurposing clinically approved cephalosporins for tuberculosis therapy. Scientific Reports. 2016 Sep 28; 6:34293. https://doi.org/10.1038/srep34293 PMID: 27678056

5. Lun S, Miranda D, Kubler A, Guo H, Maiga MC, Winglee K, et al. Synthetic Lethality Reveals Mechanisms of *Mycobacterium tuberculosis* Resistance to β-Lactams. mBio. 2014 Oct 31; 5(5):e01767–14. https://doi.org/10.1128/mBio.01767-14 PMID: 25227469

6. Corsello SM, Bittker JA, Liu Z, Gould J, McCarren P, Hirschman JE, et al. The Drug Repurposing Hub: a next-generation drug library and information resource. Nat Med. 2017 Apr 7; 23(4):405–8. https://doi.org/10.1038/nm.4306 PMID: 28388612

7. Altaf M, Miller CH, Bellows DS, O'Toole R. Evaluation of the *Mycobacterium smegmatis* and BCG models for the discovery of *Mycobacterium tuberculosis* inhibitors. Tuberculosis (Edinb). 2010 Nov; 90 (6):333–7.

8. Abrahams KA, Cox JAG, Spivey VL, Loman NJ, Pallen MJ, Constantinidou C, et al. Identification of Novel Imidazo[1,2-a]pyridine Inhibitors Targeting *M. tuberculosis* QcrB. PLoS One [Internet]. 2012 Dec 31 [cited 2018 Jun 26]; 7(12). Available from: https://www.ncbi.nlm.nih.gov/pmc/articles/PMC3534098/

9. Gurcha SS, Usha V, Cox JAG, Fütterer K, Abrahams KA, Bhatt A, et al. Biochemical and structural characterization of mycobacterial aspartyl-tRNA synthetase AspS, a promising TB drug target. PLoS ONE. 2014; 9(11):e113568. https://doi.org/10.1371/journal.pone.0113568 PMID: 25409504

10. Collins LA, Torrero MN, Franzblau SG. Green Fluorescent Protein Reporter Microplate Assay for High-Throughput Screening of Compounds against *Mycobacterium tuberculosis*. Antimicrob Agents Chemother. 1998 Feb; 42(2):344–7. PMID: 9527783

11. Zhang null, Chung null, Oldenburg null. A Simple Statistical Parameter for Use in Evaluation and Validation of High Throughput Screening Assays. J Biomol Screen. 1999; 4(2):67–73. https://doi.org/10.1177/108705719900400206 PMID: 10838414

12. McDonnell G, Russell AD. Antiseptics and Disinfectants: Activity, Action, and Resistance. Clin Microbiol Rev. 1999 Jan 1; 12(1):147–79. PMID: 9880479

13. Boostanfar R, Jain JK, Mishell DR, Paulson RJ. A prospective randomized trial comparing clomiphene citrate with tamoxifen citrate for ovulation induction. Fertil Steril. 2001 May; 75(5):1024–6. PMID: 11334921

14. Khovidhunkit W, Shoback DM. Clinical effects of raloxifene hydrochloride in women. Ann Intern Med. 1999 Mar 2; 130(5):431–9. PMID: 10068418

15. Andersen PH. The dopamine inhibitor GBR 12909: selectivity and molecular mechanism of action. Eur J Pharmacol. 1989 Aug 3; 166(3):493–504. PMID: 2530094

16. Favrot L, Grzegorzewicz AE, Lajiness DH, Marvin RK, Boucau J, Isailovic D, et al. Mechanism of inhibition of *Mycobacterium tuberculosis* antigen 85 by ebselen. Nat Commun. 2013; 4:2748. https://doi.org/10.1038/ncomms3748 PMID: 24193546

17. Chan C-Y, Prudom C, Raines SM, Charkhzarrin S, Melman SD, De Haro LP, et al. Inhibitors of V-ATPase proton transport reveal uncoupling functions of tether linking cytosolic and membrane domains of V0 subunit a (Vph1p). J Biol Chem. 2012 Mar 23; 287(13):10236–50. https://doi.org/10.1074/jbc.M111.321133 PMID: 22215674

18. Syriopoulou VP, Harding AL, Goldmann DA, Smith AL. In vitro antibacterial activity of fluorinated analogs of chloramphenicol and thiamphenicol. Antimicrob Agents Chemother. 1981 Feb; 19(2):294–7. PMID: 6957162

19. He S, Zhou Z, Liu Y, Cao Y, Meng K, Shi P, et al. Effects of the antibiotic growth promoters flavomycin and florfenicol on the autochthonous intestinal microbiota of hybrid tilapia (*Oreochromis niloticus* ♀ × *O. aureus* ♂). Arch Microbiol. 2010 Dec; 192(12):985–94. https://doi.org/10.1007/s00203-010-0627-z PMID: 20844867

20. Arsic B, Barber J, Čikoš A, Mladenovic M, Stankovic N, Novak P. 16-membered macrolide antibiotics: a review. Int J Antimicrob Agents. 2018 Mar; 51(3):283–98.

21. Salomonsson P, Gottberg L, Heilborn H, Norrlind K, Pegelow KO. Efficacy of an oral antihistamine, astemizole, as compared to a nasal steroid spray in hay fever. Allergy. 1988 Apr; 43(3):214–8. PMID: 2897804

22. Mah FS, O'Brien T, Kim T, Torkildsen G. Evaluation of the effects of olopatadine ophthalmic solution, 0.2% on the ocular surface of patients with allergic conjunctivitis and dry eye. Curr Med Res Opin. 2008 Feb; 24(2):441–7. https://doi.org/10.1185/030079908X261078 PMID: 18167176

23. Pipkorn P, Costantini C, Reynolds C, Wall M, Drake M, Sanico A, et al. The effects of the nasal antihistamines olopatadine and azelastine in nasal allergen provocation. Ann Allergy Asthma Immunol. 2008 Jul; 101(1):82–9. https://doi.org/10.1016/S1081-1206(10)60839-3 PMID: 18681089

24. Tardioli S, Buijs J, Gooijer C, van der Zwan G. pH-dependent complexation of histamine H1 receptor antagonists and human serum albumin studied by UV resonance Raman spectroscopy. J Phys Chem B. 2012 Mar 29; 116(12):3808–15. https://doi.org/10.1021/jp206409d PMID: 22372713

25. McCaleb ML, Maloff BL, Nowak SM, Lockwood DH. Sulfonylurea effects on target tissues for insulin. Diabetes Care. 1984 Jun; 7 Suppl 1:42–6.

26. Pontiroli AE, Alberetto M, Bertoletti A, Baio G, Pozza G. Sulfonylureas enhance in vivo the effectiveness of insulin in type 1 (insulin dependent) diabetes mellitus. Horm Metab Res. 1984 Dec; 16 Suppl 1:167–70.

27. Hwang H-H, Moon P-G, Lee J-E, Kim J-G, Lee W, Ryu S-H, et al. Identification of the target proteins of rosiglitazone in 3T3-L1 adipocytes through proteomic analysis of cytosolic and secreted proteins. Mol Cells. 2011 Mar; 31(3):239–46. https://doi.org/10.1007/s10059-011-0026-6 PMID: 21347706

28. Beech DJ, MacKenzie I, Bolton TB, Christen MO. Effects of pinaverium on voltage-activated calcium channel currents of single smooth muscle cells isolated from the longitudinal muscle of the rabbit jejunum. Br J Pharmacol. 1990 Feb; 99(2):374–8. PMID: 1691676

29. Navari RM, Kaplan HG, Gralla RJ, Grunberg SM, Palmer R, Fitts D. Efficacy and safety of granisetron, a selective 5-hydroxytryptamine-3 receptor antagonist, in the prevention of nausea and vomiting

induced by high-dose cisplatin. J Clin Oncol. 1994 Oct; 12(10):2204–10. https://doi.org/10.1200/JCO. 1994.12.10.2204 PMID: 7931490

30. Singh J, Kumar R. Phentermine-topiramate: First combination drug for obesity. Int J Appl Basic Med Res. 2015; 5(2):157–8. https://doi.org/10.4103/2229-516X.157177 PMID: 26097830

31. Lin K, O'Brien KM, Trujillo C, Wang R, Wallach JB, Schnappinger D, et al. Mycobacterium tuberculosis Thioredoxin Reductase Is Essential for Thiol Redox Homeostasis but Plays a Minor Role in Antioxidant Defense. PLOS Pathogens. 2016 Jun 1; 12(6):e1005675. https://doi.org/10.1371/journal.ppat.1005675 PMID: 27249779

32. DeJesus MA, Gerrick ER, Xu W, Park SW, Long JE, Boutte CC, et al. Comprehensive Essentiality Analysis of the *Mycobacterium tuberculosis* Genome via Saturating Transposon Mutagenesis. mBio. 2017 Mar 8; 8(1):e02133–16. https://doi.org/10.1128/mBio.02133-16 PMID: 28096490

33. Sassetti CM, Boyd DH, Rubin EJ. Genes required for mycobacterial growth defined by high density mutagenesis. Mol Microbiol. 2003 Apr; 48(1):77–84. PMID: 12657046

34. Akhter Y, Thakur S. Targets of ubiquitin like system in mycobacteria and related actinobacterial species. Microbiological Research. 2017 Nov 1; 204:9–29. https://doi.org/10.1016/j.micres.2017.07.002 PMID: 28870295

35. Raghavan S, Manzanillo P, Chan K, Dovey C, Cox JS. Secreted transcription factor controls *Mycobacterium tuberculosis* virulence. Nature. 2008 Aug; 454(7205):717–21. https://doi.org/10.1038/nature07219 PMID: 18685700

36. Garbe T, Servos S, Hawkins A, Dimitriadis G, Young D, Dougan G, et al. The *Mycobacterium tuberculosis* shikimate pathway genes: evolutionary relationship between biosynthetic and catabolic 3-dehydroquinases. Mol Gen Genet. 1991 Sep; 228(3):385–92. PMID: 1910148

37. Mendonça JD de, Ely F, Palma MS, Frazzon J, Basso LA, Santos DS. Functional Characterization by Genetic Complementation of aroB-Encoded Dehydroquinate Synthase from *Mycobacterium tuberculosis* H37Rv and Its Heterologous Expression and Purification. J Bacteriol. 2007 Sep 1; 189(17):6246–52. https://doi.org/10.1128/JB.00425-07 PMID: 17586643

38. Zhang B, Zhou N, Liu Y-M, Liu C, Lou C-B, Jiang C-Y, et al. Ribosome binding site libraries and pathway modules for shikimic acid synthesis with *Corynebacterium glutamicum*. Microb Cell Fact [Internet]. 2015 May 17 [cited 2018 Jun 15]; 14. Available from: https://www.ncbi.nlm.nih.gov/pmc/articles/PMC4453273/

39. Lee M-Y, Hung W-P, Tsai S-H. Improvement of shikimic acid production in *Escherichia coli* with growth phase-dependent regulation in the biosynthetic pathway from glycerol. World J Microbiol Biotechnol. 2017 Feb; 33(2):25. https://doi.org/10.1007/s11274-016-2192-3 PMID: 28044275

40. Mawuenyega KG, Forst CV, Dobos KM, Belisle JT, Chen J, Bradbury EM, et al. *Mycobacterium tuberculosis* functional network analysis by global subcellular protein profiling. Mol Biol Cell. 2005 Jan; 16 (1):396–404. https://doi.org/10.1091/mbc.E04-04-0329 PMID: 15525680

41. Raimunda D, Long JE, Padilla-Benavides T, Sassetti CM, Argüello JM. Differential roles for the Co2+/Ni2+ transporting ATPases, CtpD and CtpJ, in *Mycobacterium tuberculosis* virulence. Mol Microbiol [Internet]. 2014 Jan [cited 2018 Jun 15]; 91(1). Available from: https://www.ncbi.nlm.nih.gov/pmc/articles/PMC3885230/

42. Schifano JM, Edifor R, Sharp JD, Ouyang M, Konkimalla A, Husson RN, et al. Mycobacterial toxin MazF-mt6 inhibits translation through cleavage of 23S rRNA at the ribosomal A site. Proc Natl Acad Sci USA. 2013 May 21; 110(21):8501–6. https://doi.org/10.1073/pnas.1222031110 PMID: 23650345

43. Domenech P, Rog A, Moolji J, Radomski N, Fallow A, Leon-Solis L, et al. Origins of a 350-Kilobase Genomic Duplication in *Mycobacterium tuberculosis* and Its Impact on Virulence. Infect Immun. 2014 Jul 1; 82(7):2902–12. https://doi.org/10.1128/IAI.01791-14 PMID: 24778110

44. Keating LA, Wheeler PR, Mansoor H, Inwald JK, Dale J, Hewinson RG, et al. The pyruvate requirement of some members of the *Mycobacterium tuberculosis* complex is due to an inactive pyruvate kinase: implications for in vivo growth. Molecular Microbiology. 56(1):163–74. https://doi.org/10.1111/j.1365-2958.2005.04524.x PMID: 15773987

45. Torrey HL, Keren I, Via LE, Lee JS, Lewis K. High Persister Mutants in *Mycobacterium tuberculosis*. PLOS ONE. 2016 May 13; 11(5):e0155127. https://doi.org/10.1371/journal.pone.0155127 PMID: 27176494

46. Pethe K, Sequeira PC, Agarwalla S, Rhee K, Kuhen K, Phong WY, et al. A chemical genetic screen in *Mycobacterium tuberculosis* identifies carbon-source-dependent growth inhibitors devoid of in vivo efficacy. Nat Commun. 2010 Aug 24; 1:57. https://doi.org/10.1038/ncomms1060 PMID: 20975714

47. Viljoen A, Dubois V, Girard-Misguich F, Blaise M, Herrmann J-L, Kremer L. The diverse family of MmpL transporters in mycobacteria: from regulation to antimicrobial developments. Mol Microbiol. 2017 Jun; 104(6):889–904. https://doi.org/10.1111/mmi.13675 PMID: 28340510

48. Rodrigues L, Villellas C, Bailo R, Viveiros M, Aínsa JA. Role of the Mmr efflux pump in drug resistance in *Mycobacterium tuberculosis*. Antimicrob Agents Chemother. 2013 Feb; 57(2):751–7. https://doi.org/10.1128/AAC.01482-12 PMID: 23165464

49. Cooper CB. Development of *Mycobacterium tuberculosis* whole cell screening hits as potential antituberculosis agents. J Med Chem. 2013 Oct 24; 56(20):7755–60. https://doi.org/10.1021/jm400381v PMID: 23927683

50. Rehren G, Walters S, Fontan P, Smith I, Zárraga AM. Differential gene expression between *Mycobacterium bovis* and *Mycobacterium tuberculosis*. Tuberculosis (Edinb). 2007 Jul; 87(4):347–59.

51. Sharma U. Current possibilities and unresolved issues of drug target validation in *Mycobacterium tuberculosis*. Expert Opinion on Drug Discovery. 2011 Nov 1; 6(11):1171–86. https://doi.org/10.1517/17460441.2011.626763 PMID: 22646985

52. Goldman RC. Why are membrane targets discovered by phenotypic screens and genome sequencing in *Mycobacterium tuberculosis*? Tuberculosis (Edinb). 2013 Nov; 93(6):569–88.

53. Cole ST. Inhibiting *Mycobacterium tuberculosis* within and without. Phil Trans R Soc B. 2016 Nov 5; 371(1707):20150506. https://doi.org/10.1098/rstb.2015.0506 PMID: 27672155

54. Catterall WA, Swanson TM. Structural Basis for Pharmacology of Voltage-Gated Sodium and Calcium Channels. Mol Pharmacol. 2015 Jul; 88(1):141–50. https://doi.org/10.1124/mol.114.097659 PMID: 25848093

55. Ouellet H, Johnston JB, Ortiz de Montellano PR. The *Mycobacterium tuberculosis* Cytochrome P450 System. Arch Biochem Biophys. 2010 Jan 1; 493(1):82–95. https://doi.org/10.1016/j.abb.2009.07.011 PMID: 19635450